

Prediction of the binding interface between monoclonal antibody m102.4 and Nipah attachment glycoprotein using structure-guided alanine scanning and computational docking

Phanthakarn Tit-oon^{1,#}, Kannan Tharakaraman^{2,3,#}, Charermchai Artpradit^{1,#}, Abhinav Godavarthi^{1,π}, Pareenart Sungkeeree¹, Varun Sasisekharan¹, Jarunee Kerdwong¹, Nathaniel Loren Miller^{2,3,4}, Bhuvna Mahajan¹, Amnart Khongmanee¹, Mathuros Ruchirawat¹, Ram Sasisekharan^{2,3,*}, and Mayuree Fuangthong^{1,*}

¹Translational Research Unit, Chulabhorn Research Institute, Bangkok, 10210, Thailand

²Koch Institute for Integrative Cancer Research, Massachusetts Institute of Technology, Cambridge, MA 02139, USA

³Department of Biological Engineering, Massachusetts Institute of Technology, Cambridge, MA 02139, USA

⁴Harvard-MIT Division of Health Sciences & Technology, Massachusetts Institute of Technology, Cambridge, MA 02139, USA

^πPresent address: Yale University, New Haven, CT 06520, USA

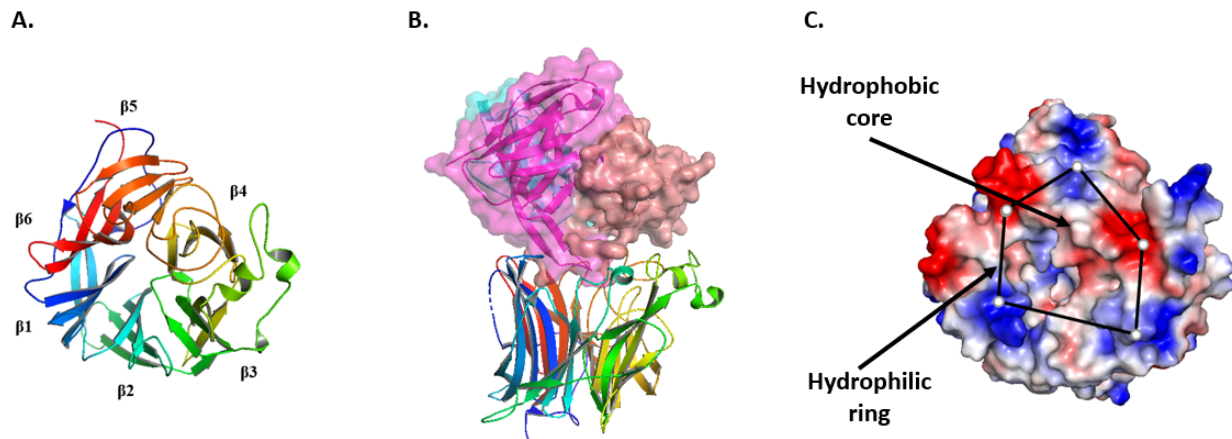
#These authors contributed equally to this work.

*To whom the correspondence should be addressed.

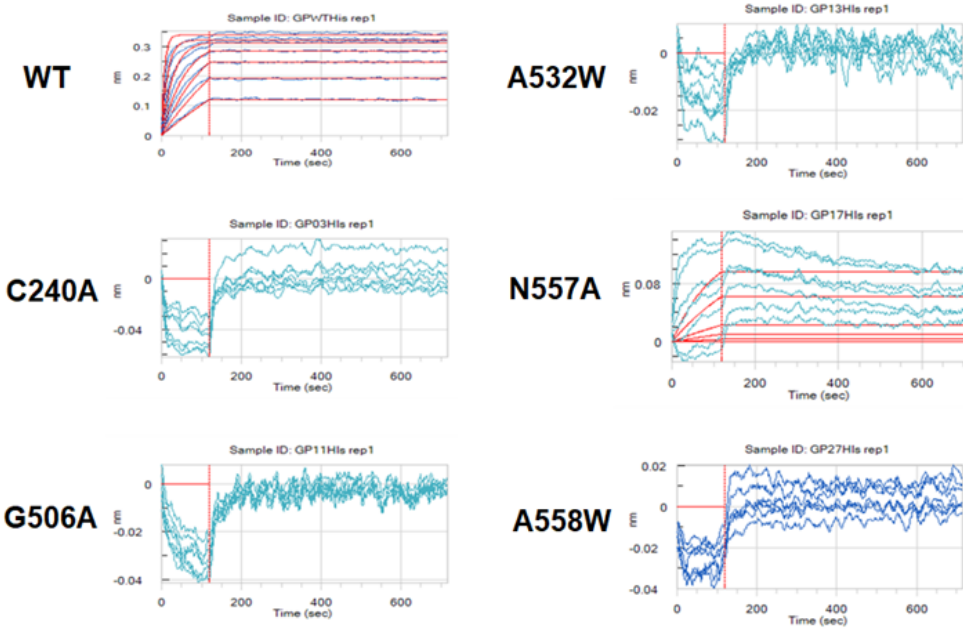
Email: mayuree@cri.or.th; Tel: +66 2 553 8535; Fax: +66 2 553 8558;

Email: rams@mit.edu; Tel: +1617 258 9494

SUPPLEMENTARY MATERIALS



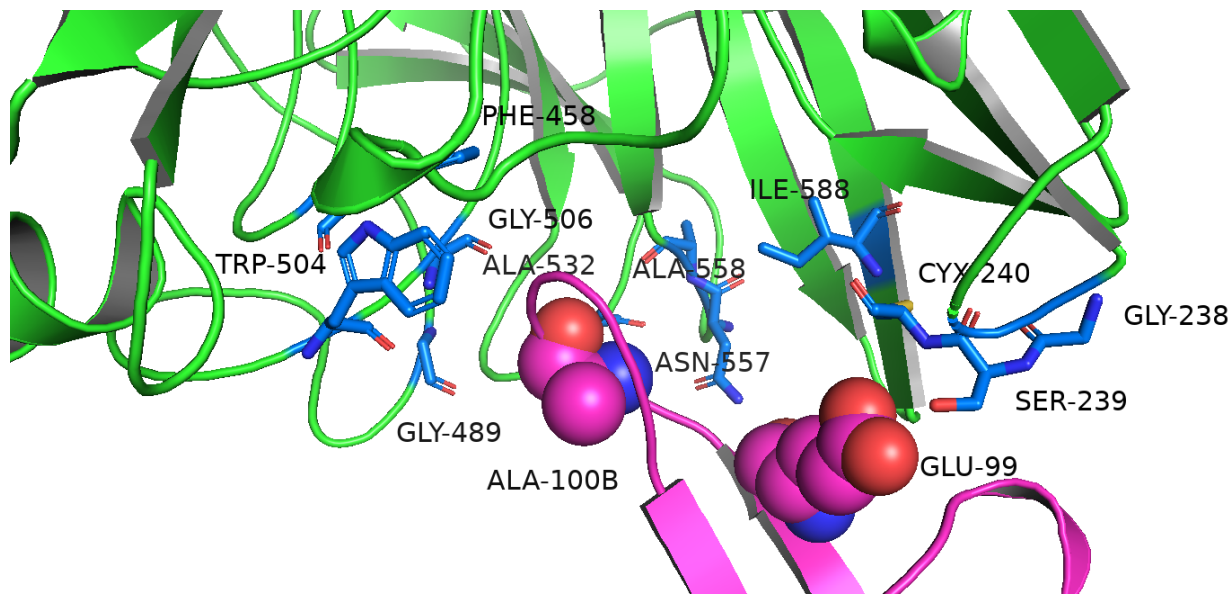
Supplementary Figure S1. Hendra GP structure and m102.3 epitope. (A) the toroidal arrangement of deglycosylated GP formed by the six beta propeller blades around a central axis (labeled). The view of GP is along the line of central axis. GP is colored in rainbow color with the N terminus in blue and the C terminus in red; (B) GP bound to m102.3 (PDB: 6CMG) and its receptor Ephrin-B2 (PDB: 6PDL). View of the GP is perpendicular to the central axis. The Fv of m102.3 is colored in magenta and cyan, respectively, whereas the receptor is in light brown. (C) m102.3 epitope consisting of hydrophobic core in the center and hydrophilic pockets at the periphery highlighted on the electrostatic surface of GP.



Supplementary Figure S2. Sensorgram data showing fit curves (shown in red) generated from Octet QKe. Kinetic assays were performed by first capturing biotinylated wild-type Nipah antibody using streptavidin biosensor. The antibody-captured biosensors were then submerged in wells containing different concentrations of G-protein for 120 sec followed by dissociation period in PBST buffer. The wild-type G-protein generates signals that fit perfectly to the curves. No fit curves were generated from the mutant G-protein with C240A, G506A, A532W, N557A, or A558W mutations.

	*
m102.3	EIVMTQSPGT PSL S GERATLSC RASQSIR STYLA WYQQKPGQAPRL LIY GASSRATGIP
m102.4	EIVMTQSPGT L SLA P GERATLSC WASQSVR NNYL WYQQKPGQAPRL VIY NGSTRATGIP
	***** *
m102.3	DRFSGSGSGTDFTLTISRLPEDFAVYYC QQYGRSP--SFGQ GTKVEIK
m102.4	DRFSGSGSGTDFTLTISRLD PEDFAVYYC QQYGNNSRRVT FGGGTKVEIK

Supplementary Figure S3. Sequence alignment between LC of m102.3 and m102.4. Amino acid differences are indicated in red. Amino acids that are different in the two chains and fall in the VH:VL interface are highlighted by an asterisk symbol. Chothia CDR loops are colored in yellow.



Supplementary Figure S4. Close-up view of m102.4-GP (NiV) interface from the docked model. The residues used as constraints for docking are highlighted by spheres (paratope) and sticks (epitope). The light chain is not seen in this orientation. The heavy chain of m102.4 and GP are colored in magenta and green, respectively.

EGVSNLVGLPNNICLQKTSNQILKPKLISYTLPPVGQSGTCITDPLLAMDEGYFAYSHLE

 RIGSCSRGVSKQRIIGVGEVLDRGDEVPSLFMTNVWTPPNPNTVYHCSAVYNNEFYYVLC

 AVSTVGDPILNSTYWSGSLLMMTRLAVKPKSNGGGYNHQQLALRSIEKGRYDKVMPYGPSG

 IKQGDTLYFP AVGFLVRTEFKYNDNSNCPITKCQYSKPENCRLSMGIRPN SHYILRSGLLK

 YNLSDGENPKVVFIEISDQRSLSIGSPSKIYDSLQPVFYQASF SWDTMIKFGDVLTVNPL


 VVNWRNNTVISRP GQSQCPRFNTCPEICWE GVY NDAFLIDRINWI SAGVFLDSN QTAENP




 VFTVFKDNEILYRAQLASEDTNAQKTITNCFLKKNKIWCISLVEIYDTGD NVIRPKLFAV

KIPEQCTA

Supplementary Figure S5. m102.3 and m102.4 epitope residues mapped on NiV GP sequence. Epitope residues that are common to both antibodies are colored in purple, whereas amino acids unique to m102.3 and m102.4 are in red and blue, respectively. Residues involved in H-bonds or salt bridge contact with both antibodies are indicated by downward pointing black arrows; Residues involved in H-bonds or salt bridge contact with m102.3 or m102.4 but not both are indicated by yellow (m102.3) and green (m102.4) arrows, respectively.

A.

NiV-GP	EGVSNLVGLPNNICLQKTSNQILKPKLISYTLPVVGQSGTCITDPLLAMDEGYFAYSHLE
HeV-GP	QGVSDLVGLPNQICLQKTTSTILKPRLLISYTLPINTREGVCTDPLLAVDNGFFAYSHLE
NiV-GP	RIGSCSRGVSQKRIIGVGEVLDRGDEVPSLFMTNVWTPPNPNTVYHCSAVYNNEFYYVLC
HeV-GP	KIGSCTRGIAKQRIIGVGEVLDRGDKVPSMFMTNVWTPPNPSTIHHCSSTYHEDFYYTLC
NiV-GP	AVSTVGDPILNSTYWSGSIMMTRLAVKPKSNGGGYNQHQLALRSIEKGRYDKVMPYGPSC
HeV-GP	AVSHVGDPILNSTSWTESLSLIRLAVRPKS DSGDYNQKYIAITKVERGKYDKVMPYGPSC
NiV-GP	IKQGDTLYFP AVGFLVRTEFKYNDNSCPITKCQYSKPENCRLSMGIRPN SHYILRSGLLK
HeV-GP	IKQGDTLYFP AVGFLPRTEFQYNDNSCPIIHCKY SKAENCRLSMGVNSKSHYILRSGLLK
NiV-GP	YNLSDGENPKVVFIEISDQRRLSIGSPSKIYDSLQGPVFYQASFSWDTMIKFGDVLT VNPL
HeV-GP	YNLSLGGDIILQFIEIADNR LTIGSPSKIYNSLGQPVFYQASYSWDTMIKLG DVDTVDPL
NiV-GP	VVNWRNNNTVISRPGQSQCPRFNTCPEICWEGVYNDALFLIDRINWISAGVFLDSNQTAENP
HeV-GP	RVQWRNNNSVISRPGQSQCPRFNVCPEVCWEGTYNDALFLIDRLNWVSAGVYLNSNQTAENP
NiV-GP	VFTVFKDNEILYRAQLASEDTNAQKTITNCFLKNKIWCISLV EYDTGDNVI RPKLFAV
HeV-GP	VFAVFKDNEILYQVPLAEDDTNAQKTITDCFLLENVIWCISLV EYDTGDSVIRPKLFAV
NiV-GP	KIPEQCTA
HeV-GP	KIPAQCSE

B.

m102.4-VH EVQVIQSGADVKKPGSSVKVSCKSSGGTFSKYAINWVRQAPGQGLEWMGGIIPILGIANY
m102.3-VH EVQLVQSGAEVKRGSSVKVSCKSSGGTFSNYAINWVRQAPGQGLEWMGGIIPILGIANY

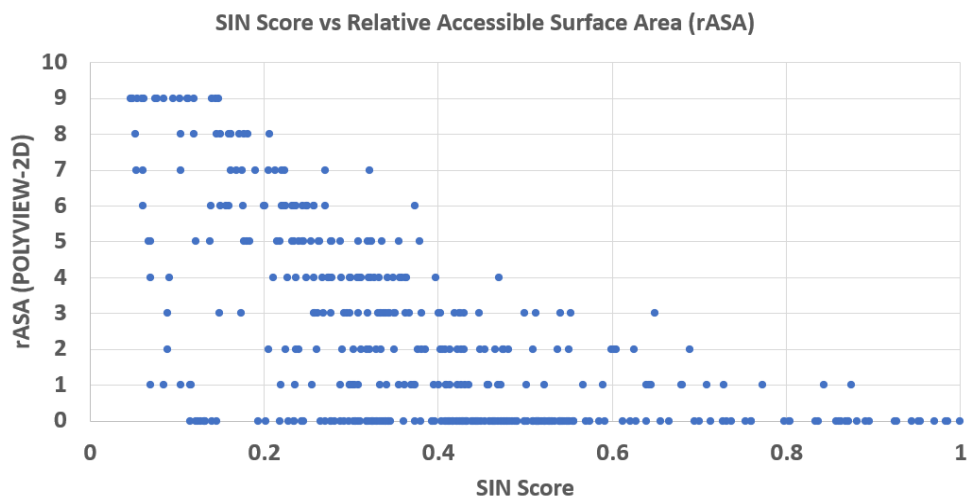
m102.4-VH AQKFQGRVTITTDESTSTAYMELSSLRSEDTAVYYCARGWGREQLAPHPSQYYYYYYGMD
m102.3-VH AQKFQGRVTITTDESTSTAYMELSSLRSEDTAVYYCARGWGREQLAPHPSQYYYYYYGMD

m102.4-VH VWGQGTTTVVSS
m102.3-VH VWGQGTTTVVSS

m102.4-VL EIVMTQSPGTLSLAPGERATLSCWASQSVRNNYLAWYQQKPGQAPRLVIYNGSTRATGIP
m102.3-VL EIVMTQSPGTPLSPGERATLSCRASQSIRSTYLAWYQQKPGQAPRLLIYGASSRATGIP

m102.4-VL DRFSGSGSGTDFTLTISRLLPEDFAVYYCQQYGN SRRVTFGGGTKVEIK
m102.3-VL DRFSGSGSGTDFTLTISRLEPEDFAVYYCQQYG--RSPSFQGTTKVEIK

Supplementary Figure S6. Residues involved in antibody–antigen interactions: m102.3-HeV (PDB:6CMG) and m102.4-NiV (pose_8193). **A.** Antibody contacts on the amino acid sequence alignment of NiV and HeV GP. Contacts made by VH and VL are colored in red and blue, respectively. **B.** Antigen contacts on the amino acid sequence alignment of VH and VL of m102.4 and m102.3, respectively. VH and VL-based contacts are colored in red and blue, respectively, consistent with the coloring employed in **A**.



Supplementary Figure S7. Scatter plot of SIN scores and solvent accessibility (expressed as relative accessible surface area calculated from POLYVIEW-2D, <http://polyview.cchmc.org/>) computed for the X-ray crystal structure of Nipah GP (PDB: 3D11).

Supplementary Table S1. Sequence of DNA primers for G-protein mutation using Gibson assembly.

Purpose	Primer ID - Sequence (5'-3')
G238A mutation	gP007-CGAAAGAACATCGCTTCGTGCTCGC gP008-GCGAGCACGAAGCGATTCTTCG
S239A mutation	gP009-AAGAACATCGCGCATGCTCGCGGG gP010-CCCGCGAGCATGCCCGATTCTT
C240A mutation	gP011-AATCGGCTCGGCTTCGCGGGGGGG gP012-CCCCCCGCGAAGCCGAGCCGATT
S241A mutation	gP013-CGGCTCGTGCACGGGGGGTGT gP014-ACACCCCCCGTGCACGAGCCG
R242A mutation	gP015-CTCGTGCTCGGCAGGGGTGTCAAAG gP016-CTTGACACCCCTGCCGAGCACGAG
L305A mutation	gP017-AGATCCTATTGCAAACCTCCACCTACTGGTCCGGTTC gP018-GAACCGGACCAGTAGGTGGAGTTGCAATAGGATCT
F458A mutation	gP019-CCAAGCGTCCGCTTCCTGGACAC gP020-GTGTCCCAGGAAGCGGACGCTTGG
P488A mutation	gP053-GGCACTGGCTCTGTCCGGCCCCGGAG gP054-CTCCCGGGCCGGACAGAGCCAGTGCC
G489A mutation	gP055-GGCACTGGCTCTGTGCGGGCCGGAG gP056-CTCCCGGGCCCGCACAGAGCCAGTGCC
Q490A mutation	gP021-CCGGCCCGGAGCCAGCCAGTGCC gP022-GGCACTGGCTGGCTCCGGCCGG
W504A mutation	gP023-GGAAATCTGCGCCGAGGGGGTGTACAATG gP024-CATTGTACACCCCTCGCGCAGATTCC
E505A mutation	gP025-AATCTGCTGGCAGGGGTGTACAATG gP026-CATTGTACACCCCTGCCAGCAGATT
G506A mutation	gP027-CTGCTGGGAGGGCTGTGTACAATG gP028-CATTGTACACAGCCTCCCAGCAG
V507A mutation	gP057-GGCGTCATTGTATGCCCTCCCAG gP058-CTGGGAGGGGGCATACAATGACGCC
T531A mutation	gP029-TAGCAACCAGGCCCGGGAGAACCC gP030-GGTTCTCCGCGGCCCTGGTTGCTA
A532W mutation	gP031-CAACCAGACCTGGGAGAACCCAG

	gP032-CTGGGTTCTCCCAGGTCTGGTTG
E533A mutation	gP033-CCAGACCGCGGCTAACCCAGTGT gP034-ACACTGGGTAGCCGCGGTCTGG
E554A mutation	gP035-ACTGGCGTCGGCTGACACCAACG gP036-CGTTGGTGTCAAGCCGACGCCAGT
D555A mutation	gP037-GGCCTCGGAGGCCACCAACGCTC gP038-GAGCGTTGGTGGCCTCCGACGCC
N557A mutation	gP039-GGAGGACACCGCCGCTAAAAGACCATTACCAACTGTTTC gP040-GAAAACAGTTGGTAATGGTCTTTGAGCGGCGGTGTCCTCC
A558W mutation	gP059-CAGTTGGTAATGGTCTTTGCCAGTTGGTGT gP060-GACACCAACTGGCAAAAGACCATTACCAACTG
Q559A mutation	gP041-CACCAACGCTGCCAAGACCATTACCAACTG gP042-CAGTTGGTAATGGTCTTGCGAGCGTTGGT
E579A mutation	gP061-GGTGTCGTAGATTGCCACGAGGGAG gP062-CTCCCTCGTGGCAATCTACGACACC
Y581A mutation	gP043-CGTGAAATGCCGACACCGGTG gP044-CACCGGTGTCGGCGATTCCACG
T583A mutation	gP045-AATCTACGACGCAGGTGATAACG gP046-CGTTATCACCTGCGTCGTAGATT
D585A mutation	gP047-CGACACCGGTGCTAACGTCAATT gP048-GAATGACGTTAGCACCGGTGTCG
N586A mutation	gP049-CACCGGTGATGCAGTCATTGCC gP050-GGCGAATGACTGCATCACCGGT
I588A mutation	gP051-TGATAACGTCGCCCCGCCCTAAACTG gP052-CAGTTAGGGCGGGGACGTTATCA
Forward primer for Gibson cloning	fw-CGGCCGCCACTGTGCTGGATTCTAGAGGATCGAACCCCTTCAC
Reverse primer for Gibson cloning	gPRv-TGTGGTGGATTCTGCAGATGAATTCATCATTCCCCGGGGAC
Forward primer for His-tag cloning	gPEcoRI-GGTGGAATTCTCTAGAGGATCGAACCCCTTCAC
Reverse primer for His-tag cloning	gPHistag-TCATCAATGATGATGATGATGTGTGCACTGCTCGGGGATC

Supplementary Table S2. Sequence of DNA primers for Nipah antibody mutation using Gibson assembly.

Purpose	Primer ID - Sequence (5'-3')
K31A mutation	Nmab007-AACCTTCTCCGCCTACGCGATTAACGGGTCCGC
	Nmab008-GCGGACCCAGTTAACCGTAGGCGGAGAAGGTT
L55A mutation	Nmab009-CATCCCAATTGCAGGGATGCCAACTACGC
	Nmab010-CTGTCCCCAGACATCCATCCCGTAGTAATAGGCGTAGTATTGG
G56A mutation	Nmab011-CCCAATTCTGGCAATGCCAACTACG
	Nmab012-CGTAGTTGGCGATTGCCAGAATTGGG
I57A mutation	Nmab013-AATTCTGGGGGCCGCAACTACGC
	Nmab014-GCGTAGTTGGCGGCCCGCAGAATT
R102A mutation	Nmab015-GGGTTGGGGAGCTGAACAGTTGGCG
	Nmab016-CGCCAACTGTTCAGCTCCCCAACCC
E103A mutation	Nmab017-TTGGGGAAGGGCCCAGTTGGCGC
	Nmab018-GCGCCAACTGGGCCCTCCCCAA
Q104A mutation	Nmab019-GGGAAGGGAAGCCTTGGCGCCCCACCCG
	Nmab020-CGGGTGGGGCGCCAAGGCTTCCCTTCC
L105A mutation	Nmab021-AAGGGAACAGGCTGCGCCCCACCCGTC
	Nmab022-GACGGGTGGGCGCAGCCTGTTCCCTT
A106W mutation	Nmab023-GGAACAGTTGTGGCCCCACCCGTCCCAATAC
	Nmab024-GTATTGGGACGGGTGGGCCACAACGTGTTCC
P107A mutation	Nmab025-ACAGTTGGCGGCCACCCGTCCC
	Nmab026-GGGACGGGTGGGCCAGCAACTGT
H108A mutation	Nmab027-GTTGGCGCCCGCTCCGTCCCAATAC
	Nmab028-TATTGGGACGGGGCGGGCGCCAAC
P109A mutation	Nmab029-GGCGCCCCACGCTTCCCAATACT
	Nmab030-AGTATTGGGAAGCGTGGGGCGCC
S110A mutation	Nmab031-GCCCCACCCGGCACAATACTACT
	Nmab032-AGTAGTATTGTGCCGGTGGGGC
Q111A mutation	Nmab033-CCACCCGTCCGCATACTACTACTATTACTAC
	Nmab034-GTAGTAATAGTAGTAGTATGCCGGACGGGTGG
Y112A mutation	Nmab035-CCCGTCCCAAGCTTACTACTATTACTACGGGATGGATG
	Nmab036-CATCCATCCCGTAGTAATAGTAGTAAGCTGGGACGGG

Purpose	Primer ID - Sequence (5'-3')
Y113A mutation	Nmab037-GTCCCAATACGCCTACTATTACTACGGGATGGATGTCTGGG Nmab046-CCCAGACATCCATCCCGTCGTAATAGTAGGCGTATTGGGAC
Y114A mutation	Nmab039-CCAATACTACGCCTATTACTACGGGATGGATGTCTGGGACAG Nmab040-CTGTCCCCAGACATCCATCCCGTAGTAATAGGCGTAGTATTGG
L55A mutation	Nmab048-CATCATCCCAGCACTGGGGATGCC Nmab047-GGCGATCCCCAGTGCTGGGATGATG
Forward primer for Gibson assembly	fw-CGGCCGCCACTGTGCTGGATTCTAGAGGATCGAACCCCTTCAC
Reverse primer for Gibson assembly	VHrv-TGTGGTGGAATTCTGCAGATTCATCATTACCCGGCGACAACGACAGTG

Supplementary Table S3. Theoretical prediction of changes in Gibbs free energy of binding ($\Delta\Delta G$) computed using mCSM-AB¹. The positions inferred by Xu *et al.*² are highlighted in yellow. As seen below, 7/13 alanine mutations reduce antigen binding, contradicting the experimentally generated data.

CHAIN	WILD_RES	RES_POS	MUT_RES	RSA	PRED_ΔΔG	Predicted Affinity Change
B	R	30	A	58.0	-0.146	Reduce
B	T	32	A	66.6	-0.658	Reduce
B	R	94	A	58.7	-1.572	Reduce
C	N	31	A	64.5	0.152	Increase
C	I	54	A	48.9	-0.336	Reduce
C	G	56	A	88.0	0.191	Increase
C	I	57	A	11.0	-0.291	Reduce
C	R	102	A	47.0	-1.662	Reduce
C	E	103	A	8.2	-1.503	Reduce
C	Q	104	A	9.9	-0.575	Reduce
C	L	105	A	0.6	0.643	Increase
C	A	106	W	0.0	-1.257	Reduce
C	P	107	A	0.1	-0.297	Reduce
C	H	108	A	9.7	0.825	Increase
C	P	109	A	3.3	0.26	Increase
C	S	110	A	32.4	0.079	Increase
C	Q	111	A	58.3	0.035	Increase
C	Y	112	A	11.4	-0.304	Reduce
C	Y	113	A	9.4	-0.951	Reduce
C	Y	114	A	8.8	-1.242	Reduce
C	Y	115	A	16.5	-1.518	Reduce

**RSA: Relative Solvent Accessibility

Supplementary Table S4. Amino acid sequences of VH and VL regions of m102.3 and m102.4 disclosed in US 2009/0214428 A1 (2009) and Xu *et al.*². Amino acid differences between the two published sources are highlighted in bold and colored in red.

Mab	Source	VH	VL
m102.3	US 2009/0214428 A1 (2009)	EV QVI QSGAD VKK P GSSV KVSCKSSGGTFS K YAINWVRQAPGQGLEWMGGIPILGIANYAQ KFQGRVTITTDESTSTAYMELSSLRSEDTVAV YYCARGWGREQ L A PHPSQ YYYYYYGMDVWGQ GTTVTVSS	EIVMTQSPGTPLSPGERATLSCRASQ SIRSTYLAWYQQKPGQAPRLLIYGASS RATGIPDRFSGSGSGTDFTLTISRLEP EDFAVYYCQQYGRSPSFGQGTKVEIK
	Xu <i>et al.</i> ²	EV QLV QSGAE VKK P GSSV KVSCKSSGGTFS N YAINWVRQAPGQGLEWMGGIPILGIANYAQ KFQGRVTITTDESTSTAYMELSSLRSEDTVAV YYCARGWGREQ L A PHPSQ YYYYYYGMDVWGQ GTTVTVSS	EIVMTQSPGTPLSPGERATLSCRASQ SIRSTYLAWYQQKPGQAPRLLIYGASS RATGIPDRFSGSGSGTDFTLTISRLEP EDFAVYYCQQYGRSPSFGQGTKVEIK
m102.4	US 2009/0214428 A1 (2009)	EV QVI QSGAD VKK P GSSV KVSCKSSGGTFS K YAINWVRQAPGQGLEWMGGIPILGIANYAQ KFQGRVTITTDESTSTAYMELSSLRSEDTVAV YYCARGWGREQ L A PHPSQ YYYYYYGMDVWGQ GTTVTVSS	EIVMTQSPGTLSIAPGERATLSCWASQ SVRNLYLAWYQQKPGQAPRLLVINYNGST RATGIPDRFSGSGSGTDFTLTISRLDP EDFAVYYCQQYGNNSRRVTFGGGTKVEIK
	Xu <i>et al.</i> ²	EV QLV QSGAE VKK P GSSV KVSCKSSGGTFS N YAINWVRQAPGQGLEWMGGIPILGIANYAQ KFQGRVTITTDESTSTAYMELSSLRSEDTVAV YYCARGWGREQ L A PHPSQ YYYYYYGMDVWGQ GTTVTVSS	EIVMTQSPGTLSIAPGERATLSCWASQ SVRNLYLAWYQQKPGQAPRLLVINYNGST RATGIPDRFSGSGSGTDFTLTISRLDP EDFAVYYCQQYGNNSRRVTFGGGTKVEIK

References

1. Pires, D. E. & Ascher, D. B. mCSM-AB: a web server for predicting antibody-antigen affinity changes upon mutation with graph-based signatures. *Nucleic Acids Res* **44**, W469-473, doi:10.1093/nar/gkw458 (2016).
2. Xu, K. *et al.* Crystal structure of the Hendra virus attachment G glycoprotein bound to a potent cross-reactive neutralizing human monoclonal antibody. *PLoS Pathog* **9**, e1003684, doi:10.1371/journal.ppat.1003684 (2013).